

Novel Super Hydrophilic Alloy Coatings by Low-energy Process

Fengyan Hou, Ian Mardon, Zhendi Yang and Chris Goode*

Cirrus Materials Science Limited

5b Target Court, Auckland 0627, New Zealand, *chris.goode@cirrusmaterials.com

ABSTRACT

We present a low-voltage, non-toxic Plasma Electrolytic Oxidation (PEO) coating technology to produce super hydrophilic surfaces on light alloys. This novel surface finishing process provides thin, adherent, and durable surfaces on light alloys at low cost with an exceptionally low energy using environmentally sustainable process. The technology is applicable to magnesium, aluminium and titanium substrates or films and operates at less than 5% of traditional PEO process power. Functional PEO surfaces with high hardness (>7.66Gpa) and superhydrophilicity (<5° contact angles) are widely applicable in medical and consumer electronics.

Keywords: Hydrophilicity, Plasma Electrolytic Oxidation (PEO), Light Metal, hardness, sustainable, low energy, medical, Electronic

1 INTRODUCTION

Light metal substrates with super hydrophilic properties are of great interest to medical and consumer electronics applications. Plasma Electrolytic Oxidation (PEO) is a surface-treatment process which creates a protective layer on light metal substrates by anodic oxidation. PEO treatments produce desirable mechanical, corrosion, and morphological properties. While magnesium, aluminium, and titanium alloys are among the most common light metals subjected to PEO surface treatments [1], recent reviews also report the use of PEO surface treatments for copper, zinc, tantalum, and niobium substrates [2].

Traditional PEO processes are energy intensive. PEO occurs by applying high voltages in an electrolyte between a target electrode and a stable cathode via direct current (DC), pulsed DC or alternating current (AC). The high voltages generate a plasma state localized at the arc discharge points leading to the formation of adherent mixed oxide coatings on the light metal substrates. Factors such as processing voltages, current density, temperature, and electrolyte composition influence the performance of PEO-treated surfaces. Of these the chemical composition of a PEO electrolyte plays a significant role in both the formation and performance of coatings [3]. For example, silicate and phosphate compounds in electrolytes are responsible for the enhanced hardness of PEO treated surfaces [4,5].

In the current study Cirrus Materials Science aimed to design a sustainable low power PEO process for light metal surface modification. Here, we report a PEO surface

modification process that produces adherent and mechanically robust coatings on Mg, Al and Ti alloys using low energy and a benign silicate-based organo-alkaline electrolyte.

2 EXPERIMENTAL

Samples of AZ80 magnesium, 6061 aluminium and T1 titanium alloys were first abraded with emery papers, rinsed with water, and then cleaned in an alkaline degreasing solution. The degreasing bath comprised 20 g/L NaCO₃, 20 g/L Na₂PO₄, 20 g/L Na₂SiO₃, and 3 g/L commercially available OP-10 surfactant. The simple pre-treatment design removed both organic contaminants and excessively thick native oxides from the sample surfaces. Deionised water rinses prepared the samples for PEO treatment.

Sample PEO processing adopted a common bath, comprising 70 g/l NaOH, 60 g/L Na₂SiO₃, 10 g/L Na₃C₆H₅O₇, 6 mL/L H₂O₂, and 0.05 milli mol/L sodium dodecyl sulphate. Two sample sets, 'A' and 'B' were prepared, with the "B" set processed in a bath additionally containing, 4.9 mL/L aminophenol. PEO processes were conducted at ~25°C for 15 min in all cases, using stainless steel counter electrodes. Table 1 summarises the constant current densities and associated processing voltages adopted for the various substrates.

Table 1. PEO parameters for different substrates

Substrates	Set Current Density	PEO Voltage
AZ80 Mg	1A/dm ²	<160V
6061 Al	4A/dm ²	<160V
T1 Ti	4A/dm ²	<120V

A Rigaku XtaLAB Synergy-s single crystal X-ray diffractometer equipped with a Cu K_α source was used to collect phase and composition data on the oxidized sample surfaces. The XRD patterns were analysed using the Materials Explorer application on Materials Project open database [6].

Pt sputtering using a Quorum Tech Q150T prepared the sample for morphology imaging and characterisation using an FEI XL30 SEM equipped with a 30 kV field emission gun.

Deionized water (DIW) contact angle measurement determined surface wettability. Measurements analysed images taken from the side and top of approximately 0.0083mL of DIW deposited on a horizontal sample surface.

Direct measurement of contact angles from the side images was possible for angles higher than 20°. Lower contact angle measurements, especially those lower than 10°, adopted an estimation of the contact angle from spherical analysis using the average droplet surface diameter measured from the top image.

Nanoindentation testing on prepared cross sections of the ceramic oxide coatings provided hardness performance data.

3 RESULT AND DISCUSSION

3.1 Synthesis

Voltage vs time graphs (Figure 1) show the low energies required to develop compact oxide films on the light metal alloy substrates. Initially, the current limited voltage rises during growth of the compact, oxide barrier. When the

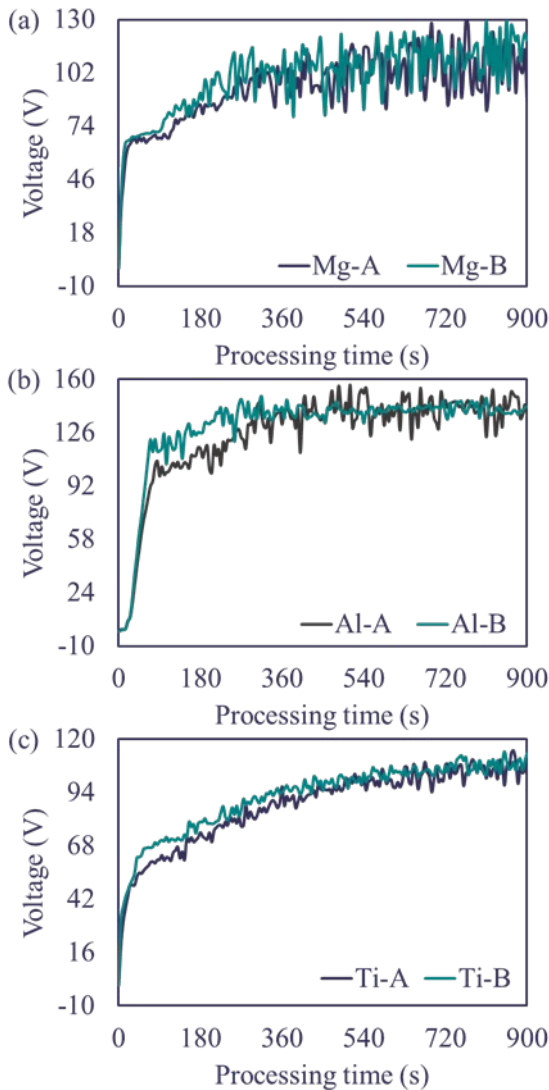


Figure 1. Voltage vs. time graphs of PEO treatment of a) Magnesium, b) Aluminium, and c) Titanium alloys in Cirrus' PEO bath.

coating thickness reaches a critical thickness, small arcs, associated with barrier layer breakdown voltage, spread over the barrier layer surface. These arcs are associated with the formation of high-energy plasma flow channels where an exchange of substrate and bath materials occurs and oxides and silicates form building the coating.

3.2 Structure and composition of coatings

Scanning electron microscope (SEM) images (Figure 2) of the surfaces of treated alloys demonstrated that the addition of an aminophenol to the PEO electrolyte significantly changed the coating surface morphologies. Mg-A and Al-A and Ti-A samples PEO-treated in an organo-silicate electrolyte and exhibit pores and surface cracks, which are typical of such ceramic oxide coatings [7]. Analysis of higher magnification surface and cross-sectional SEM images, not shown here, determined the dimensions of some coating features mentioned in the following paragraphs.

Mg-A coating (Figure 2 a) exhibits plateau-like features and pores of varying dimensions. The surface cracks appear to propagate into the coating by a few nanometers. Mg-B coatings (Figure 2 b) exhibit a basalt-like morphology with uniformly distributed pores on the surface. The pore dimensions range from 10 nm to around 2.00 μm .

Al-A coating (Figure 2 c) shows sporadically distributed pores of <50 nm and a bi-layer surface morphology (clearly observed in cross-section images). The coating also exhibits surface cracks that appear to propagate in the coating. Al-B coatings (Figure 2 d) show increased pore density and thus increased porosity. The average pore dimensions are larger when compared to Al-A and range from 10 nm – ~1.5 μm .

The pore sizes of Ti-A (Figure 2 e) ranged from <1.00 μm to 3.00 μm . The surface for Ti-B (Figure 2 f) has cracks and pores integral to oxidized layers but the pore-structure here appears denser.

In this study, we observe that the addition of aminophenol to PEO electrolyte refines the porosity of Mg-B, Al-B and Ti-B coatings. The electrolyte modification enabled a greater control in pore dimensions on those metal surface due to the surfactant-like behaviour of aminophenol. Our hypothesis is that reduction in the gas bubble dimensions is due to variations in arc-discharge intensity, temperatures and pressures in the discharge channels caused by aminophenolic modification of the PEO electrolyte. The changes in electrolyte properties also appear to increase the uniformity and density of discharge channels on the surface.

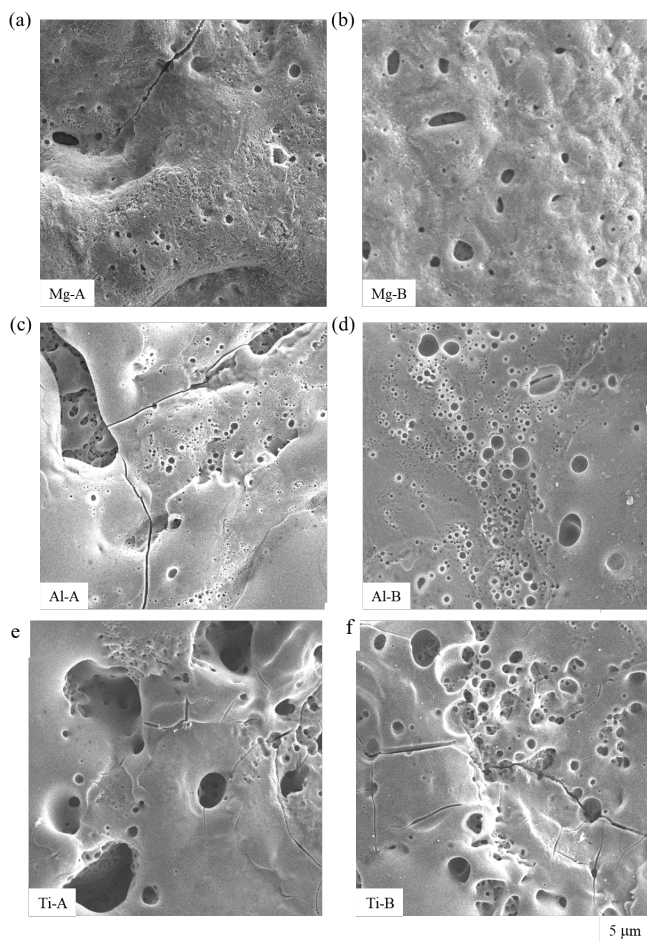


Figure 2. Surface morphology of (a) Mg-A. (b) Mg-B. (c) Al-A. (d) Al-B. (e) Ti-A and (f) Ti-B.

Figure 3 shows the X-ray diffraction (XRD) patterns collected for the PEO-treated Mg-A coating (Figure 3 a) which comprise peak associated with oxides, hydroxides, and silicates of magnesium. The XRD pattern for Mg-B (Figure 3 b) shows the presence of not only oxides, hydroxides, and silicates of Mg but also characteristic peaks associated with the presence of Mg_3N_2 and MgO_xN_y in the coating. We hypothesize that the arc-energies generated during aminophenol-enhanced PEO treatment of AZ80 alloys are sufficiently high for the formation of Mg_3N_2 in the coating [8]. The appearance of magnesium oxynitride in the coating suggests that the localized arc energies are capable of nitriding MgO.

XRD patterns for Al-A and B and Ti-A and B (not shown) are similar, thus indicating that aminophenol modification of the electrolyte has little influence on the crystallographic properties of these coatings. Addition of aminophenol to the PEO bath is responsible for the nitrides, detected on Al-B and Ti-B.

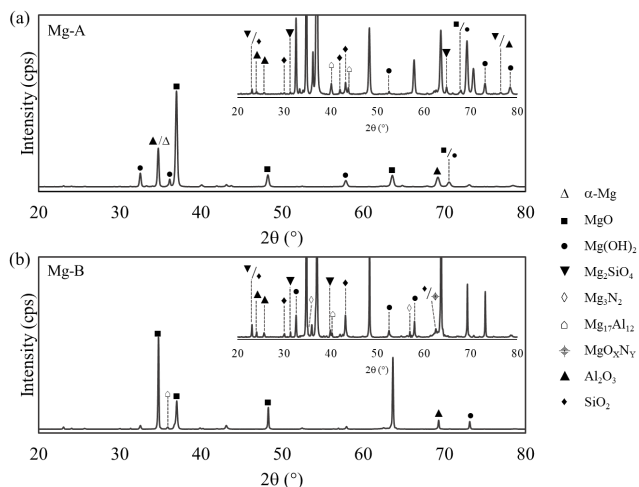


Figure 2: XRD patterns for PEO-treated AZ80 (a) Mg-A and (b) Mg-B

3.3 Coating Performance

Hydrophilic property

Contact angles with deionised water (DIW) were measured on both the raw and PEO processed Al and Ti surfaces. Generally, the PEO process significantly reduced the DIW contact angle and produced superphyla surfaces.

The raw Al substrate has a contact angle with DIW of 85° (Figure 4). PEO processing significantly reduced the DIW contact angle, which became 0.5° (Figure 5). Analysis of the surface contact angle evolution over a two-week period demonstrated that the PEO processed Al surface remained super-hydrophilic (Figure 6).



Figure 3. Contact angle with DIW on as received Al



Figure 4. Contact angle with DIW on PEO processed Al

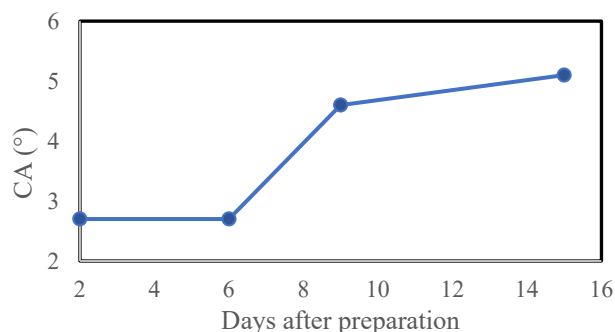


Figure 5. Super-hydrophilic contact angles over time on PEO processed Al

Contact angle measurements on Ti T1 substrates followed a similar trend. Before processing the pre-treated Ti, had a contact angle with DIW of 45° (Figure 7). Post PEO processing the Ti surface became super-hydrophilic, with a contact angle of $\sim 1.7^\circ$ (Figure 8 a), and remained super hydrophilic over a 3-week analysis period (Figure 8 b).



Figure 6. Contact angle with DIW on as received Ti

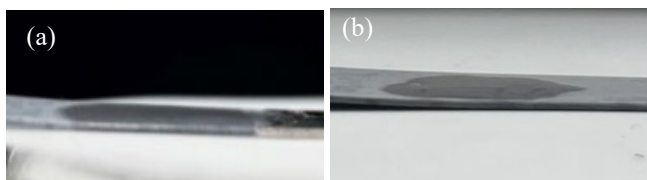


Figure 8. Contact angle with DIW on PEO processed Ti (a) as prepared and (b) 3 weeks after preparation

Hardness

Table 2 summarises the results of nanoindentation tests, performed on the coating cross-sections, evaluated the mechanical behaviour of Mg-A, Mg-B, Al-A and Al-B and Ti-A and Ti-B.

Table 2. Nano-hardness of Mg, Al and Ti samples treated from various processes

Substrates	Nano-hardness (GPa)		
	Raw	A	B
AZ80 Mg	1.06	7.66	8.58
6061 Al	1.81	5.73	7.03
Ti Ti	4.43	6.63	7.12

The PEO process reported in this paper improved the surface hardness by at least 7 times for Mg alloys, by at least

3 times for Al alloys, and at least 1.5 times for Ti alloys. Untreated AZ80 alloy exhibits a nano hardness of 1.06 GPa. Mg-A coatings exhibit 7.66 GPa and Mg-B coatings, 8.58 GPa. Untreated Al6061 alloy exhibits 1.81 GPa. Al-A coatings exhibit 5.73 GPa and Al-B coatings exhibit 7.03 GPa. Bare Ti-alloys possess hardness of 4.43GPa. Ti-A coatings exhibit 6.63 GPa and Ti-B coatings exhibit 7.12 GPa. The improved hardness of the treated alloys is due to the formation of a robust oxide layer reinforced by silicate particle incorporation. The incorporation of nitrides and oxynitrides into the coating composition improved the hardness of Mg-B by 12% and Al-B by 22% and Ti-B by 7.4% respectively.

4 CONCLUSION

In conclusion, we achieved reliable protection of light metal substrates using a low energy PEO process with eco-friendly electrolytes. We demonstrated a facile method to incorporate carbon and nitrogen-compounds into oxide coatings of Mg, Al, and Ti to achieve long lived super hydrophobic surfaces. The PEO coatings exhibit crystalline properties and are composed of metal oxides, silicates and oxynitrides. Low-energy PEO (<160V) surface modification can form super-hydrophilic surfaces with enhanced mechanical properties through nitridation of the coatings, which may be desirable for medical and consumer electronics applications.

REFERENCES

- [1] F. C. Walsh *et al.*, Transactions of the IMF. 87, 122-135, 2009.
- [2] A. Sobolev, M. Zinigrad, and K. Borodianskiy, Surface & Coatings Technology, 408, 10, 2021.
- [3] Y. Zhang, *et al.*, Int. J. Electrochem. Sci. 13 (8), 7923-7929. 2018.
- [4] A. Pardo, P. Casajus, M. Mohedano and A. E. Coy, Applied Surface Science, 255 (15), 6968-6977, 2009.
- [5] E. Matykina, *et al.*, Transactions of Nonferrous Metals Society of China 27 (7), 1439-1454, 2017.
- [6] A. Jain, *et al.*, APL Materials 1 (1), 011002, 2013.
- [7] G. B. Darband, *et al.*, J. Magnes. Alloy, 5 (1), 74-132, 2017.
- [8] A. Shanaghi, B. Mehrjou, and P. K. Chu, J. Biomed. Mater. Res. Part A, 16.